

Baryon Number Transport in High Energy Nuclear Collisions

M. Gyulassy¹, V. Topor Pop^{1,2}, S.E. Vance¹

¹Physics Department, Columbia University, New York, N.Y. 10027

²Institute for Space Sciences, P.O.Box MG-6, Bucharest, Romania

Abstract: Recent SPS data on the rapidity distribution of protons in p+S, p+Au and S+S collisions at 200 AGeV and preliminary Pb+Pb collisions at 160 AGeV are compared to HIJING and VENUS calculations as well as to predictions based on the Multi-Chain Model (MCM). The preliminary Pb data suggest that a linear dependence of the proton rapidity shift as a function of the nuclear thickness, as first observed in p+A reactions, may apply up to Pb+Pb reactions. The observed rapidity dependence of produced hyperons in both p+A and A+A reactions however cannot be explained in terms of such models without introducing additional non-linear effects.

1 Introduction

Preliminary data on baryon number transport in $Pb + Pb \rightarrow p, \bar{p}, \Lambda, \bar{\Lambda}$ [1, 2, 3, 4, 5] at 160 AGeV has become available. These data are of interest as tests of nuclear stopping power [6]. The first estimates of the baryon stopping power of heavy nuclei was made by Busza and Goldhaber [7] based on the A dependence of $p + A \rightarrow p + X$ data at fixed $p_{\perp} = 0.3$ GeV. Baryon stopping power refers to the transport of baryon number away from the nuclear fragmentation regions and is measured in terms of the single inclusive rapidity distribution of protons and hyperons. In ref. [8], the estimates were refined by taking into account exact Glauber geometry and applying the Multi-Chain Model (MCM) parameterization of baryon number transport. For a review of the average rapidity loss for $p + p$, and $A + A$ collisions at beam momenta 11.6, 14.6 and 200 GeV/c per nucleon see ref.[9]. Until recently, the most complete information on nuclear stopping power was limited to the $p + Ag$ data of Toothacker et al. [10].

Systematic data from heavy-ion collisions [1, 2, 3, 4, 5, 11, 12, 13] provide new information about the nuclear stopping power. Important information about baryon inelasticity also comes from the analysis of veto and transverse energies distributions [14]-[18].

As summarized in [6], baryon number transport is one of the key observable that has been debated for some time in connection with the ongoing search for nonlinear dynamical phenomena in nuclear reactions. One source of nonlinear behavior may arise if a quark-gluon plasma is formed in such reactions. In this connection, the observed strangeness enhancement and hyperon production data [1, 5, 11, 14],[19]-[22] have stimulated particular interest[23, 24]. In [25] it was pointed out, however, that the unusual difference

*This work was supported by the Director, Office of Energy Research, Division of Nuclear Physics of the Office of High Energy and Nuclear Physics of the U.S. Department of Energy under Contract No. DE-FG02-93ER40764.

between hyperon production in $p + p$ and minimum bias $p + S$ may reflect more the onset of novel *non-equilibrium* dynamical mechanisms.

The breakdown of the linear dependence of baryon rapidity shifts as a function of the mean collision number, $\nu \sim A^{1/3}$, is one of the obvious places to look for new phenomena. The linearity assumption underlying MCM and many Monte Carlo event generators is motivated by the phenomenology of string formation and fragmentation[26, 27, 28, 29]. Such linear behavior is also expected if the radiative energy loss per unit length is a constant in nuclei[30].

Several recent theoretical developments have raised, however, new possibilities for nonlinear dynamics associated with baryon number transport. In one development [31], a non-linear energy loss of gluons in nuclei was predicted as a function of the nuclear thickness, L

$$\Delta E_g \approx \frac{1}{8} \alpha_s N_c L \langle p_{\perp}^2 \rangle_L \sim 15 \text{ GeV} \left(\frac{L}{10 \text{ fm}} \right)^2 . \quad (1)$$

This energy loss could, under appropriate conditions, lead to enhanced rapidity shifts of hadrons passing through nuclei.

A second possible source of nonlinearity was suggested in ref.[32] based on the Rossi-Veneziano[33] baryon-junction Regge exchange model. This mechanism can give rise to large rapidity shifts of the baryon number offset by only a modest enhancement of the forward final pion rapidity density. This mechanism could even modify significantly baryon transport up to RHIC energies because the assumed junction Regge intercept, $\alpha_J(0) = 0.5$, leads to a slow suppression of this mechanism with increasing energy ($\propto s^{-1/4}$).

An even more exotic baryon transport mechanism was proposed in [34] based on a variant[35] of the above baryon-junction exchange model. In that variant the junction trajectory is assumed to have unit intercept and thus leads to an energy independent uniform rapidity density component of the inclusive proton yield.

Given the new data and the above theoretical speculations, it is appropriate to take analyze carefully the available information on baryon transport and hyperon production. We therefore take into account the older $p, \bar{p} + Ag$ data at 100A GeV [10], the new $p + A$ [21], [1] at 200 GeV, the $S + A$ at 200 AGeV[1, 20, 21], and the $Pb + Pb$ data at 160A GeV [2, 4, 5, 12, 22]. In a previous paper, we concentrated on the anomalous hyperon production processes[25]. Here we concentrate on the proton rapidity shifts in nuclear collisions. We test whether nuclear stopping power extrapolates linearly from $p + A$ to $Pb + Pb$. In this analysis we recall the predictions of the Multi-Chain Model[8] (MCM) as well as utilize the Monte Carlo HIJING1.3 [28] and VENUS4.12 [29] models as in [25].

2 The Multi Chain Model

Since the HIJING and VENUS models were discussed extensively in [25], we recall here only the essential elements of the MCM to be used in the present analysis.

The single inclusive proton rapidity distribution in $B + A \rightarrow p + X$ reactions is given

in general by Glauber theory as

$$\frac{dN^{BA \rightarrow pX}}{dy} = \sum_{m=1}^B \sum_{n=1}^A P_{BA}(m, n) Q_{m,n}(y) , \quad (2)$$

where the tedious but well understood nuclear geometry is separated from the multiple collision dynamics encoded in the functions, $Q_{m,n}(y)$. The probability that a group of m projectile nucleons multiple scatter with n target nucleons is given by

$$P_{BA}(m, n) = \int \frac{d^2\mathbf{b}}{\sigma_{AB}} \mathcal{B}(\mathbf{b}) \int \frac{d^2\mathbf{s}}{\sigma_{in}} P_B(m, N_B(\mathbf{s})/B) P_A(n, N_A(\mathbf{b} - \mathbf{s})/A) , \quad (3)$$

where $P_A(m, x) = C_{m,A} x^m (1-x)^{A-m}$ is the binomial distribution. The mean number of inelastic collision in nucleus A at impact parameter \mathbf{b} in terms of the diffuse nuclear density and inelastic pp cross section, $\sigma_{in} \approx 32$ mb by $N_A(\mathbf{b}) = \sigma_{in} \int dz \rho_A(z, \mathbf{b})$. The impact parameter profile function \mathcal{B} is included above to account for the experimental trigger bias (e.g. veto or transverse energy cuts). For minimum bias events, $\mathcal{B} = 1$. For a given profile, the total reaction cross section is

$$\sigma_{AB} = \int d^2\mathbf{b} \mathcal{B}(\mathbf{b}) \left(1 - (1 - \int d^2\mathbf{s} N_B(\mathbf{s}) N_A(\mathbf{b} - \mathbf{s}) / (AB\sigma_{in}))^{BA} \right) . \quad (4)$$

The main simplifying assumption of the MCM is that of independent fragmentation:

$$Q_{m,n}(y) \approx m Q_n(Y - y) + n Q_m(y) , \quad (5)$$

where Y is the rapidity difference between the projectile and target. As emphasized in [8], this linear superposition ansatz is far from obvious, and one of the important questions awaiting the recent heavy ion data is whether this breaks down for sufficiently heavy nuclear collisions[6]. With this ansatz the rapidity distribution simplifies to

$$\frac{dN^{BA \rightarrow pX}}{dy} = r_B W_B \sum_{n=1}^A P_{B/A}(n) Q_n(Y - y) + r_A W_A \sum_{m=1}^B P_{A/B}(m) Q_n(m) , \quad (6)$$

where $r_B = (Z_B f + N_B(1 - f))/B$ is the fraction of projectile baryons that fragment into protons, and where W_B is the average number of wounded baryons in nucleus B :

$$W_B = \int \frac{d^2\mathbf{b}}{\sigma_{AB}} \mathcal{B}(\mathbf{b}) \int \frac{d^2\mathbf{s}}{\sigma_{in}} N_B(\mathbf{s}) \{1 - [1 - N_A(\mathbf{b} - \mathbf{s})/A]^A\} \quad (7)$$

and $P_{B/A}(n)$ is the fraction of them that interact with n target nucleons. Typically[8], the fraction of incident protons that remain protons is $f \approx 0.53$ away from the diffractive peaks.

What remains then to be determined are the dynamical fragmentation functions, $Q_n(y)$, specifying the rapidity distribution of target baryons that have suffered n inelastic interactions. For $n = 1$, i.e., $p + p$, the MCM assumes the simple form

$$Q_1(y, \alpha) = e^{-y} , \quad (8)$$

as consistent with the flat dN/dx distribution observed away from the diffractive peak ($x \sim 1$). For $n \geq 2$ the multiple collision contribution to baryon rapidity transport is parameterized in the MCM model by a one parameter class of functions:

$$Q_n(y, \alpha) = \left(\frac{\alpha}{\alpha - 1}\right)^{n-1} \left[e^{-y} - e^{-\alpha y} \sum_{m=0}^{n-2} \frac{1}{m!} (\alpha - 1)^m y^m \right]. \quad (9)$$

These functions arise using a scaling algorithm[8] in which the probability density that spectator partons retain a fraction z of the total light-cone momentum after an inelastic interaction is $\alpha z^{\alpha-1}$. This ansatz implies a geometric scaling of the spectator energy fraction moments $\langle z^p \rangle_{F_n} = (\alpha/(\alpha + p))^n$ and a linear scaling of the mean rapidity shift with collision number n :

$$\langle y \rangle_n = 1 + (n - 1)/\alpha. \quad (10)$$

Detailed fits to the Barton et al[36] $p + A \rightarrow p + X$ data at 100 GeV, gave $\alpha = 3 \pm 1$. Other models[7] can also achieve good fits to the existing $p + A$ data with different parameterizations. For example, a recent fit with the constituent quark model was presented in [37]. The advantage of the MCM approach is in its simplicity, reducing the problem of the nuclear stopping power to one phenomenological parameter, α . Recall that the naive incoherent cascade limit corresponds to $\alpha = 1$, leading to one unit rapidity shift per interaction. The empirical $\alpha = 3$ arises because the inelasticity per interaction inside nuclear targets is reduced by the finite formation time of secondary fragments.

We note that the scaling approximation used above certainly breaks down for lower energies where the rapidity gap, Y , between projectile and target becomes $\lesssim 3$. In the following we simply cutoff Q_n with a $\theta(Y - y)$ factor and normalize Q_n in that finite interval. In [8] a slightly different finite energy cutoff prescription was used. Fortunately, for $E_{lab} > 100$ GeV such cutoff effects are unimportant.

At the pp level we can test for the possibility of novel baryon junction transport[32]. If the probability of junction exchange is ϵ_J and its Regge intercept is α_J , then Q_1 would be modified from (8) to

$$Q_1(y) = (1 - \epsilon_J)e^{-y} + \epsilon_J(1 - \alpha_J)e^{-(1-\alpha_J)y}. \quad (11)$$

Actually, the contribution of junction exchange close to the fragmentation regions is not well determined and the above form may only apply for $y \gg 1$. Given the above form, the final $p - \bar{p}$ rapidity distribution in the cm with a rapidity gap $2Y$ would be

$$\frac{dN^{pp \rightarrow pX}}{dy} = r_p \left((1 - \epsilon_J) \frac{\cosh(y)}{\sinh(Y)} + \epsilon_J(1 - \alpha_J) \frac{\cosh((1 - \alpha_J)y)}{\sinh((1 - \alpha_J)Y)} \right). \quad (12)$$

In figure 1, the valence proton, $p - \bar{p}$, distribution from pp collisions at 400 GeV[38] is shown compared to MCM and HIJING. These same data were used to test VENUS in [29]. The mid-rapidity yield is underestimated by HIJING by a factor of two, while the VENUS proton fragmentation scheme fits better[29]. Both VENUS and HIJING over-predict the forward $y \sim 6$ yields. The excellent agreement with the simple MCM form, $\cosh(y - Y)$, with $r_p = 0.53$ leaves little room for exotic baryon exchange contributions at this energy.

At higher energies, $\sqrt{s} = 53A\text{GeV}$, Ref.[32] finds evidence for taking $\epsilon_J > 0$. However, Fig. 1 demonstrated conventional baryon trajectory exchange reproduces accurately the observed valence proton rapidity distribution at this lower energy. This point is important since in [32] it was hinted that at SPS energies such conventional mechanism at least as expressed in the Dual Parton Model [27] could not reproduce the experimental stopping power in nucleus-nucleus reactions. Part of the problem in DPM and HIJING discrepancy with $pp \rightarrow pX$ data can be traced to the assumed diquark fragmentation schemes. We return to this point in section 5.

3 Baryon transport in $p + A$

In Figure 2. we compare calculations with the 100 GeV $p, \bar{p} + Ag \rightarrow pX$ data[10]. Part (a) shows the dN/dy distribution in the projectile fragmentation domain ($\Delta y < 2$) and the higher but narrower dN/dy distribution in the target fragmentation domain ($\Delta y > 4$). Both the MCM prediction (with $\alpha = 3$) and the VENUS model are seen to reproduce the leading proton distribution within the experimental errors. HIJING leads to a similar mean rapidity shift but is distributed more narrowly about the mean. This is due to the default diquark fragmentation scheme in JETSET[26] which is used in HIJING. VENUS does not use the JETSET scheme and has been adjusted to reproduce the flat fragmentation region[29].

The target region is isolated in part (b) through the $\bar{p} + A \rightarrow p + X$ channel. Since MCM and HIJING only account for the wounded baryons, the narrow nuclear enhancement around the target rapidity ($\Delta y = 5.3$) can only be reproduced by VENUS, which incorporates final state interactions. However, the main interest is the probability that a target proton emerges near the projectile rapidity $\Delta y \sim 1$ in Fig.2b. While the data fluctuate greatly in that region, they are consistent with the expected exponential fall from eq.(8). As in Figure 1, there is little need here to invoke a junction exchange contribution[32] with intercept 1/2 that would lead to a $\exp[y/2]$ rather than the conventional $\exp[y]$ tail in this opposite fragmentation region.

In Fig. 2c the projectile fragmentation region is isolated through the $\bar{p} + A \rightarrow \bar{p} + X$ channel. The MCM model is consistent with the data while both HIJING and VENUS tend to overestimate this distribution just as both over-predicted the $y \sim 6$ region. In Fig. 2d the A dependence of the MCM baryon distribution is illustrated. We recall that in MCM, $dN/dy(y \rightarrow 0) = r_p P_A(1)$ is completely fixed by the geometrical probability that the projectile proton interacts only once and the probability, r_p that the proton remains a proton after fragmentation. (As in Fig.1 , $r_p = 0.53$ [8] here.)

In Figure 3, we compare the models to preliminary $p + A$ data reported from NA35[1]. Parts (a) and (c) show the $p - \bar{p}$ distributions for S and Au targets respectively. The peculiar feature in (a) relative to previous data is that in this case HIJING best reproduces the projectile fragmentation peak in $p + S$. In this case the MCM distribution is too flat. The mean rapidity shift in all three models is about the same ($\Delta y \approx 1.3$) in accord with previous systematics [7], but the narrow peak at $y = 5$ is unexpected for minimum bias events given in Figures 1 and 2. The new $p + Au$ minimum bias data in part (d) also

indicates a greater stopping power than encoded in the models HIJING and VENUS with a significantly suppressed yield beyond $y > 4$ and an enhanced yield below $y < 4$. The calculated minimum bias rapidity shift in MCM is $\Delta y \approx 2$ while the data indicate perhaps $\Delta y \approx 2.5$. Such a large rapidity shift is achieved only in the extrapolated most central $p + A$ reactions in the older data[36].

There appears therefore to be a discrepancy between the data in Fig.3a and the older data[36]. Unfortunately the data in Fig.2 have too low statistical significance to settle this problem. Note that in these plots the unobserved target fragmentation regions are artificially cutoff below $y < 0.5$. Upcoming $p + A$ data with NA49 will hopefully clarify this ambiguous situation.

As seen in Fig. 3, the net $\Lambda - \bar{\Lambda}$ hyperon distributions is even in greater disagreement with respect to both VENUS and HIJING calculations. In ref.[25] the absence of Λ fragments beyond $y > 5$ in $p + S$ and beyond $y > 4$ in $p + Au$ was emphasized to be anomalous relative to $pp \rightarrow \Lambda$ data and $\mu p \rightarrow \Lambda$ data previously analyzed in [25, 29]. In those p target reactions, the Λ rapidity distribution closely mirrors the proton fragment distribution with reduced normalization due to the expected suppression of strange flavor production. The suppression of the forward Λ relative to forward p cannot be accounted for even with the double string mechanism added into VENUS. The lack of any measured Λ 's beyond $y > 4$ in minimum bias $p + Au$ is especially peculiar. We thus re-confirm that hyperon transport in $p + A$ is anomalous relative to non-strange baryons, and is already evident in minimum bias $p + S$ reactions, where on the average, the incident protons only interacts with two target nucleons.

4 Baryon Number Flow in $A + A$

We turn next to the distribution of valence baryons in $A + A$ collisions at SPS for which some preliminary data have become available from NA49[2, 4, 12] and NA44[3]. As noted in [6] data on nuclear stopping power in $Pb + Pb$ collisions is long awaited as a critical test of nuclear transport models and to constrain the maximal baryon densities achieved in such reactions.

Figure 4 compares the spectrum of pion and participants protons in $S + S$ at 200 AGeV [20] and $Pb + Pb$ reactions at 160 AGeV [2, 3, 12]. The various data sets from NA35 for $S + S \rightarrow \pi^- + X$ correspond to different centrality triggers [20], with the higher one corresponding to a more severe veto trigger cut (see reference [20] for more details). We see that the negative pion rapidity densities are well accounted for by both HIJING [28] and VENUS [29]. This is largely due to the fact that the pion distribution simply grows linearly with the atomic number between $S + S$ and $Pb + Pb$. The centrality trigger was implemented in the above calculations via an impact parameter cut of $b < 1$ fm. For the MCM calculation the impact parameter cut for $Pb + Pb$ was taken to be 3.3 fm to simulate more closely the 5-6% centrality trigger[2].

The significant central rapidity minimum in the $p - \bar{p} dN/dy$ predicted by HIJING is traced back here to the excess central minimum in pp in Fig.1 characteristic of FRITIOF type string models. By adjusting the fragmentation functions that fit the pp central

rapidity region better, VENUS, can avoid the suppression of the mid-rapidity protons that HIJING and other models using JETSET predict. On the other hand, MCM, which fits well both the pp and the pA data as shown in Figs. 1,2, is seen to reproduce well the central $p - \bar{p}$ distribution in both SS and $PbPb$.

Figures 4a,c demonstrate the insensitivity of the pion distribution to the underlying baryon number flow. In particular, the rather large difference between the proton distribution in HIJING and VENUS in Fig.4d is contrasted by the much more modest difference of the pion distributions in Fig.4c. As we show in section 5, the forward energy flux is a more sensitive measure of the energy degradation difference between the models.

Our main conclusion is that the central region baryon number transport in $A + A$ can be well understood on the basis of a linear extrapolation of the mean rapidity shift as a function of the collision number as given by eq.(6). The main difference between the valence distribution functions in pA and BA arises simply from the variation of the Glauber geometrical probabilities of multiple interactions in the different projectile and target combinations.

An important caveat to the above conclusion is the somewhat narrower rapidity distribution of the most recent analysis[4] on $Pb + Pb \rightarrow (p - \bar{p})$ than reported in [2]. This difference is shown by comparing the solid dots to the solid triangles in Fig.4d. If in the final analysis, the [4] narrow distribution is confirmed, then the $Pb + Pb$ baryon stopping power would have to be regarded as anomalous relative to $p + A$ [7, 10] has well since then an additional 1/2 unit rapidity shift would be required over that predicted by MCM nor VENUS. In [4], it was estimated that the net integrated proton number implied by the recent analysis is close to $2 \times Z(Pb)$. This itself is peculiar since the one expects more protons from $n \rightarrow p$ exchange. At this time the central rapidity region is most reliable since another experiment [3] and alternate TOF measurements converge within errors in that region and are closest to the theoretical expectations based on $p + A$ systematics. Nevertheless, it will be important to follow up the high rapidity tails assess the significance of the present preliminary indications.

Figure 5 shows that modulo the extreme fragmentation regions, the enhanced hyperon yield in SS and SAu can be understood in terms of the VENUS model double string hypothesis and in strong disagreement with extrapolated yields using HIJING from pp reactions. The factor of two enhancement of hyperon production is already needed in minimum bias pS in Fig. 3b, but is even more evident in Fig.5. The excess rapidity shift of the hyperons relative to non-strange baryons is also clear from Fig.5 since the peaks are shifted approximately one unit of rapidity further than those calculated for protons in Fig.4b. This enhanced hyperon transport is currently not explained by any of these models. In the preliminary $Pb + Pb$ analysis[5] a truly astonishing sharply peaked Λ distribution was suggested with $dN(\lambda)/dy = 23 \pm 3$. If confirmed, $\Lambda/p \approx 0.7$ would be one of the most remarkable signature of novel phenomena in the heavy ion reaction.

Since the MCM can account for at least the central region, non-strange baryon flow up to SPS energies, it is of interest to extend the calculation up to RHIC energies, where the rapidity gap opens up to over 10 units. In Figure 6 we show the expected valence proton distribution expected at RHIC compared to present energies for $Pb + Pb$ at $b < 1$ fm central collisions. From this we estimate that the central baryon density that can be

conservatively expected at RHIC is

$$\rho_B \approx \frac{3}{2} \frac{dN^{p-\bar{p}}}{dy} \frac{1}{r_p \pi R^2 \tau} \approx \rho_0 (0.7 \text{ fm}/\tau) , \quad (13)$$

where $\rho_0 \approx 0.17 \text{ fm}^{-3}$.

5 Energy Degradation versus Baryon Number Transport

A question related to baryon transport is the rapidity distribution of energy lost by the valence baryons. Do a few high rapidity pions carry away the missing baryon energy or is the energy shared between a large number of slower pions? Data on the forward veto calorimeter distribution shed useful light on this problem as was first emphasized in the analysis of WA80 data[39].

In Figure 7 the veto calorimeter cross section is shown for NA35 $S + S$ [14] (Fig. 7b) and NA49 $Pb + Pb$ [15] (Fig. 7d). The veto calorimeter measures energy in a narrow angular cone with $\Delta\theta \sim 0.3^\circ$. In both cases the well known horseback shape follows directly from Glauber geometry of spectator nucleons and is reproduced by VENUS and HIJING. However, the tail region at small E_{VETO} is sensitive to the energy degradation in central collisions. In Fig. 7 a,c the dependence of the contribution from collisions in the range $b < 1 \text{ fm}$ is illustrated in both VENUS and HIJING models. For central collisions, VENUS, in closer agreement with the data, displays greater energy degradation than HIJING.

The correlation of the mean veto energy with the total multiplicity, participant nucleon number and impact parameter in both models is shown in Fig. 8. Fig. 8d demonstrated the equivalence of the Glauber multiple-collision geometry used in both models. However, the other parts show that the veto energy is systematically higher (and hence the energy degradation lower) in the HIJING model. Figure 9 shows the analogous correlations for the Pb+Pb reaction.

While at first sight it may seem obvious that greater baryon stopping implies greater energy degradation, we show in Figure 10 that such a correlation cannot be taken *a priori* for granted given the uncertainty in the soft hadronization mechanism. In an older version of the diquark fragmentation scheme used in the version JETSET6.3[40] it was possible to modify the baryon fragmentation through the parameter $p = PAR(52)$ in the LUDAT1 common block. This parameter controls the momentum fraction of the junction J quark of a given diquark through

$$f(x_J) \propto x_J(1 - x_J)^p , \quad \langle x_J \rangle = \frac{2}{3 + p} \quad (14)$$

Increase of the parameter p beyond the default value $p = 1$ obviously softens the diquark fragmentation function and leads to larger baryon rapidity shifts. Using the ATTILA[41] version of the FRITIOF model[26] it is possible to explore the consequences of varying

this nonperturbative model parameter. The results are shown in Fig.10. We note that HIJING1.3[28] utilizes the new particle conventions of JETSET7.2[42], which are incompatible with the previous version 6.3. Unfortunately, in version 7.2 and higher, it is no longer possible to vary `par(52)`. The once option (`ihpr2(11)=2` in HIJING) to switch to the JETSET “popcorn” fragmentation scheme unfortunately leads to even greater discrepancy with respect to $pp \rightarrow pX$ data in Fig.1.

It is seen from Fig.10 that setting $p = 10$ for $Pb + Pb$ reactions leads to a very large modification of the net proton distribution, from the default minimum to a maximum. In this case $\langle x_J \rangle \approx 0.15$. In comparison, the MCM model leads to $\langle x \rangle = (\alpha/(1 + \alpha))^{n-1}/2 \sim (3/4)^3/2 \approx 0.2$ for central $Pb + Pb$ where the *average* number of collision per wounded nucleon is $\langle \nu \rangle \approx 4.2$. The MCM curve from Fig.4 is also shown for comparison.

We find, therefore, that softening the diquark fragmentation can lead to similar baryon number transport as MCM and VENUS. Recall that VENUS incorporates also a diquark breakup component in its fragmentation scheme. The important point here is not that a variation of p can simulate more closely the baryon transport in VENUS and MCM, but that this model shows a priori no correlation between the energy degradation and baryon number transport can be assumed. In Fig. 10b the veto calorimeter cross section is essentially independent of p parameter. In this model the missing baryon energy is carried away into the veto calorimeter by a few high rapidity pions that fragment from the leading quark. The mechanism in VENUS that leads to greater energy degradation with increasing baryon rapidity shift is the dynamical assumption of the occurrence of a double rather than a single string in a fraction of the events that lead to large baryon rapidity shifts. From this analysis we conclude that the diquark mechanism of JETSET must be replaced in HIJING to enable the simultaneous reproduction of both the rapidity distributions and the veto calorimeter systematics.

6 Conclusions

One of our conclusions is that the nuclear stopping power, extracted from $p+A$ data[7] and extrapolated linearly via the MCM model to nuclear collisions, accounts quantitatively for the observed mid-rapidity baryon number transport up to central $Pb + Pb$ reactions at 160 AGeV AGeV[1, 2, 3]. The main difference between the valence baryon distribution functions in pA and BA arises from the variation of the Glauber geometrical probabilities of multiple interactions. The pion rapidity distributions are insensitive to the details of the energy degradation associated with the baryon number transport and are proportional to the wounded nucleon number.

The forward veto calorimeter data is a sensitive probe of energy degradation and amplifies subtle variations of the angular distribution of fast pions. The HIJING model and its variants (with modified diquark fragmentation via eq.(14), cannot account for the veto cross sections. VENUS, on the other hand, reproduces both the baryon distribution and veto cross sections well. It remains to find out whether the novel double string mechanism assumed in VENUS is critical to both observations, or could the veto cross sections simply reflect an enhanced final state interaction effect in the spectator regions.

In any case, the strongly non-linear dependence of hyperon production definitely requires new dynamical mechanism that becomes operative already in $p+S$ reactions. The VENUS model identifies this new mechanism with the double string formation.

However, the large hyperon rapidity shift in the preliminary $p+S$ and $S+S$ data remain unaccounted for even with the present double string mechanism in VENUS 4.12. Not only is there a large enhancement of midrapidity hyperon production in $p+S$ and $S+S$, but there is a rapidity mismatch between strange and non-strange baryons. Only the non-strange baryon transport is linear with $A^{1/3}$ within the present errors of the experiments. The provocative preliminary data of [4, 5] also point in the same direction.

Hyperon production in $Pb+Pb$ is however not entirely settled experimentally. The NA44 data in Fig. 4d include a substantial fraction of the net hyperon production while in NA49, the hyperon contribution has been subtracted out. The present experimental and systematic errors are too large to rule out a midrapidity maximum of the net baryon distribution. Our conclusion on linearity of baryon transport is thus subject to the above caveats. The present analysis in any case demonstrates the necessity of modifying the baryon fragmentation part of HIJING, FRITIOF, and DPM models.

7 Acknowledgments

One of us (VTP) thanks M. Morando and R. A. Ricci for kind hospitality at INFN - Sezione di Padova, Italy, where part of the calculations were performed. Discussions with J.Harris, P. Jacobs, D. Kharzeev, B. Kopeliovich, S. Margetis, W. Willis, and N. Xu are gratefully acknowledged. We also thank K. Werner for permission to use the VENUS code.

References

- [1] D. Röhrich et al., Proceedings of the Conference on Strangeness in Hadronic Matter, 15 - 17 May 1996, Budapest, Hungary (edited by T.Csörgó, P.Lévai, J. Zimányi), APH N.S., Heavy Ion Phys. **4** (1996) 71 .
- [2] T.Wienold et al., Proceedings of the Twelfth International Conference on Ultra-Relativistic Nucleus-Nucleus Collisions, Heidelberg, Germany, 20 -24 May, 1996 (edited by P.Braun Munzinger, R. Stock, H. Stöcker), Nucl. Phys. **A610** (1996) 76c.
- [3] N. Xu et al., Nucl. Phys. **A610**, 175c (1996); J. Bearden et al, Phys.Lett. B372 (1996) 339.
- [4] P. Jacobs (NA49 Collab) , Proc. ICPAQGP97, Jaipur, India, March 17-21,1997; <http://na49info.cern.ch/cgi-bin/wwwd-util/NA49/NOTE?123>.
- [5] C. Bormann (NA49 Collab), Proc. Stangeness in Quark Matter 97, Santorini, Greece, April 14-18,1997; <http://na49info.cern.ch/cgi-bin/wwwd-util/NA49/NOTE?124>.

- [6] M. Gyulassy ,Proc. of Eleventh International Conference on Ultra-Relativistic Nucleus-Nucleus Collisions , Quark Matter '95 (Monterey,California,USA 9-13 January 1995) eds A. M. Poskanzer,J. W. Harris and L. S. Schroeder, Nucl. Phys. **A590** (1995) 197c.
- [7] W. Busza and A. Goldhaber, Phys. Lett. 139B (1984) 235; W. Busza, R. Ledoux, Ann. Rev. Nucl. Part. Sci., ed. J. D. Jackson, **38**(1989) 119.
- [8] S. Date, M. Gyulassy and H. Sumiyoshi, Phys. Rev. **D32** (1985) 619.
- [9] F. Videbaek,Ole Hansen ,Phys. Rev. **C52**(1995) 2684.
- [10] W. S. Toothacker et al., Phys. Lett. **B197**(1987) 295.
- [11] A. Bamberger et al., Z. Phys. **C43**(1989) 25.
- [12] M. Gazdzicki et al., Nucl. Phys. **A590**(1995) 197c.
- [13] J. W. Harris, Proceedings of the 12 th Winter Workshop on Nuclear Dynamics, Snowbird, Utah (1995); John W. Harris, Berndt Muller, DUKE-TH-96-105, Ann.Rev.Nucl.Part.Sci 46 (1997) 71-107. e-Print Archive: hep-ph/9602235.
- [14] J. Bächler et al., Z. fur Phys. **C52**(1991) 239.
- [15] S. Margetis et al., Nucl. Phys. **A590**(1995) 355c.
- [16] T. Alber et al., Phys. Rev. Lett. **75** (1995) 3814.
- [17] H. Lohner et al., Z. Phys. **C38**(1988) 97.
- [18] R. Albrecht et al., Z. Phys. **C55**(1992) 539.
- [19] J. Bartke et al., Z. Phys. **C48**, 191 (1990).
- [20] J. B'achler et al., Phys. Rev. Lett. **72**(1994) 1419.
- [21] T. Alber et. al.,Z. Phys. **C64**(1994) 195.
- [22] T.Alber et al., Phys. Lett. **B366**, 56 (1996).
- [23] P. Koch, B. Muller and J. Rafelski Phys. Rep. **C142**(1986) 167.
- [24] M. Gaździki and U. Heinz, Phys. Rev. **C54** (1996) 1496.
- [25] V. Topor Pop, et al., Phys. Rev. **C52**, 1618 (1995); M. Gyulassy, V. Topor Pop, X. N. Wang, Phys. Rev. **C54** (1996) 1497.
- [26] B. Andersson, et al., Nucl. Phys. **B281** (1987) 289; Comp. Phys. Commun. **43**(1987) 387.

- [27] A. Capella, U. Sukhatme, C. I. Tan and J. Tran Thanh Van ,Phys. Rep. **236**(1994) 225.
- [28] X. N. Wang and M. Gyulassy, Phys. Rev. **D44**(1991) 3501; Phys. Rev. **D45** (1992) 844 ; Comp. Phys. Comm.,**83**(1994) 307 .
- [29] K. Werner, Phys. Rep. **232**, 87 (1993).
- [30] M.Gyulassy and X.N. Wang, Nucl. Phys. B420 (1994) 583-614; X.N. Wang, M. Gyulassy, M. Plümer, Phys.Rev.D51 (1995) 3436-3446.
- [31] R. Baier, Yu.L. Dokshitser, A.H. Mueller, S. Peigne, D. Schiff; Nucl.Phys.B484 (1997) 265; Nucl.Phys.B483 (1997) 291;Nucl.Phys.B478(1997)577.
- [32] D. Kharzeev, Phys.Lett.B378 (1996)238.
- [33] G.C. Rossi and G. Veneziano, Nucl.Phys. B123 (1977) 507; Phys.Rept. 63 (1980) 153.
- [34] B. Kopeliovics and B. Povh, hep-ph/9607486.
- [35] E. Gatsman anf S. Nussinov, Phys.Rev. D22 (1980) 624.
- [36] D. S. Barton et al., Phys. Rev. **D27**(1983) 2580.
- [37] T.C. Choi, M.Maruya, and F. Takagi, Phys. Rev C55 (1997) 848.
- [38] M. Aguilar-Benitez et al, LEBC-EHS Collab, Z. Phys. C50 (1991) 405.
- [39] S. Sorensen et al.,Z. Phys. **C38**(1988) 3 .
- [40] T. Sjöstrand, JETSET6.3 version manual, LU-TP-86-22 (1986), unpublished.
- [41] M. Gyulassy, CERN-TH-4794 (1987), GSI-87-42 (1987), unpublished; The code AT-TILA together with JETSET6.3 used to obtain Fig.10 are available through email request.
- [42] T. Sjostrand, Comp. Phys. Comm. **82**(1994) 74 ; 39 (1986) 347; Hans-Uno Bengtsson, T. Sjostrand Comput.Phys.Commun.46 (1987) 43.

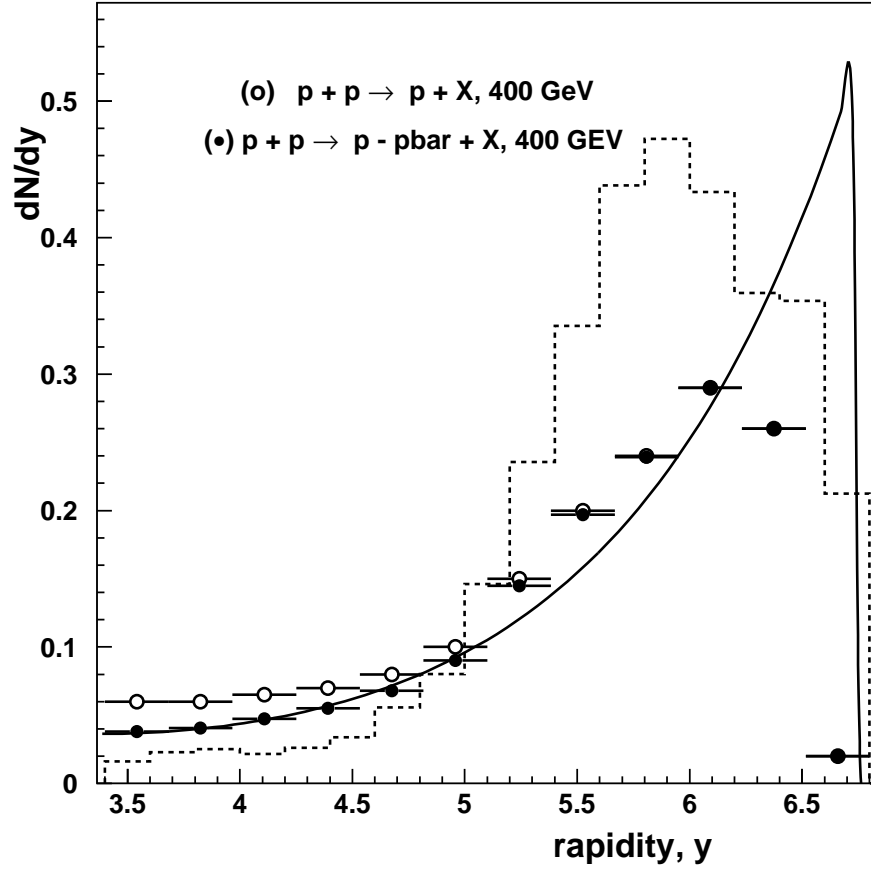


Figure 1: Solid circles show the valence proton rapidity distribution ($dn_p/dy - dn_{\bar{p}}/dy$) in non-diffractive pp reactions at 400 GeV [38], and open circles show the net proton distribution. The solid curve corresponds to the default Multi Chain model[8] fragmentation function eq. (8) with $r_p = 0.53$. The dashed histogram is obtained using the HIJING1.3 [28] code.

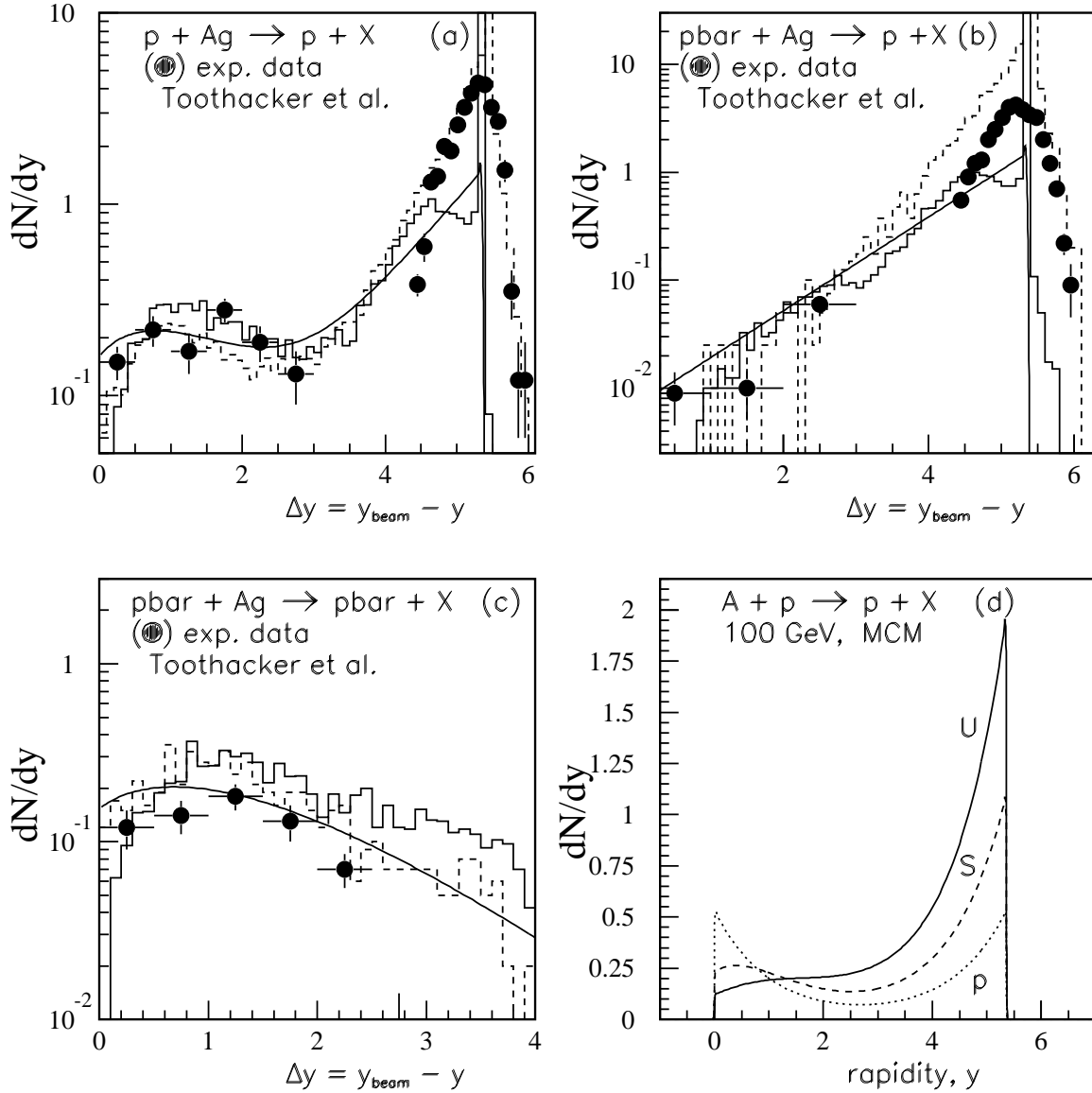


Figure 2: Baryon transport in minimum bias $p, \bar{p} + Ag$ reactions at 100 GeV. The solid and dashed histograms display HIJING and VENUS model results respectively as a function of $\Delta y = y_{\text{beam}} - y$ with $y_{\text{beam}} = 5.4$. The smooth curve is the result of the Multi-Chain Model. The channel shown in part (b) isolates the target fragmentation region while (c) isolates the projectile fragmentation region. Part (d) shows the predicted A dependence of the proton rapidity distribution with $\alpha = 3$ in the MCM.

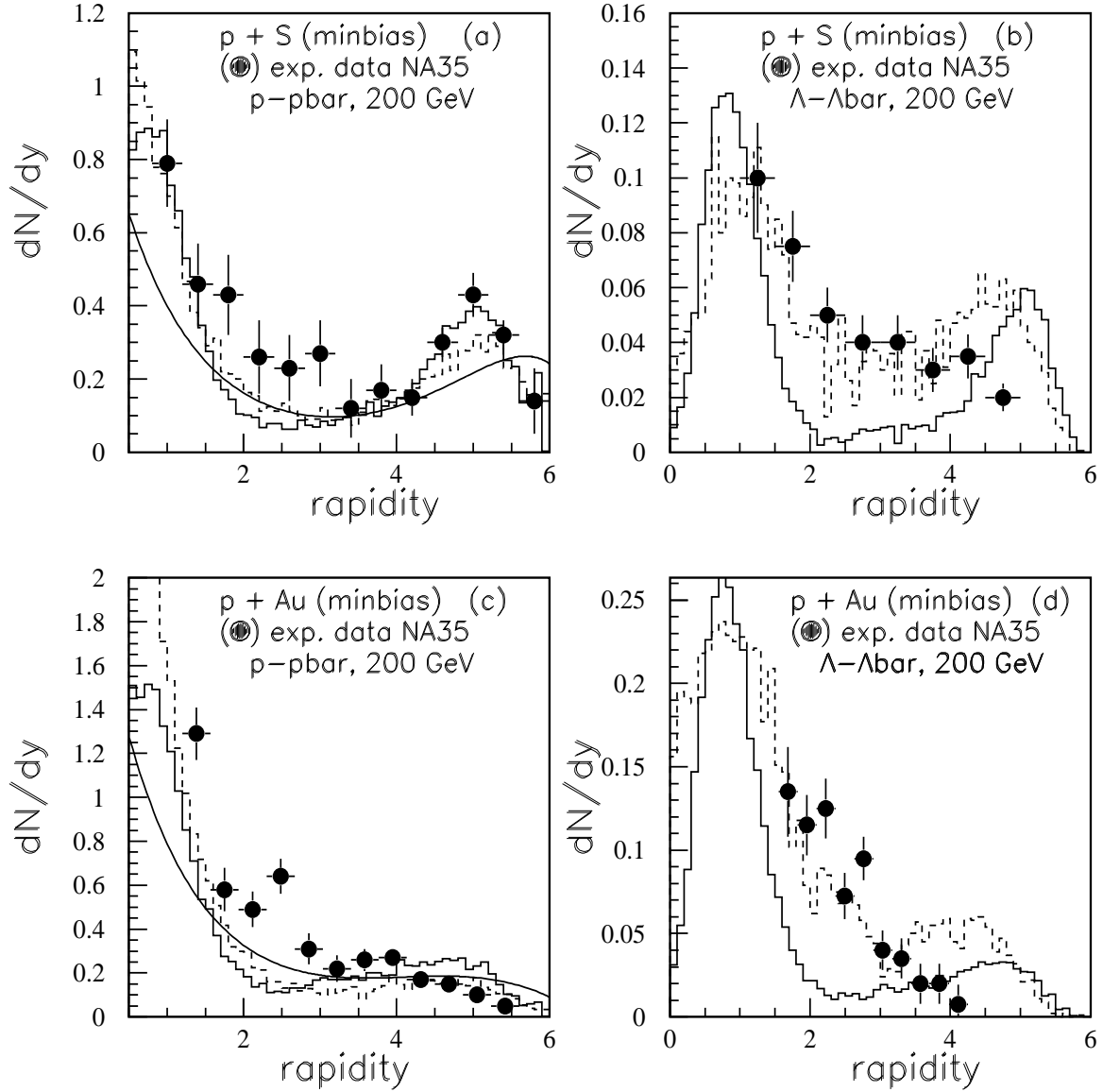


Figure 3: Baryon number transport in minimum bias $p + S, Au$ reactions[1] at 200 GeV. Curves are as in Fig.2. Here y is the laboratory rapidity with $y > 0.5$. In parts (a) and (c) the $p - \bar{p}$ distributions are shown while parts (b) and (d) correspond to the $\Lambda - \bar{\Lambda}$ distributions. Note that the data indicate significantly greater rapidity shifts hyperons relative to non-strange-baryons in contrast to both VENUS and HIJING calculations.

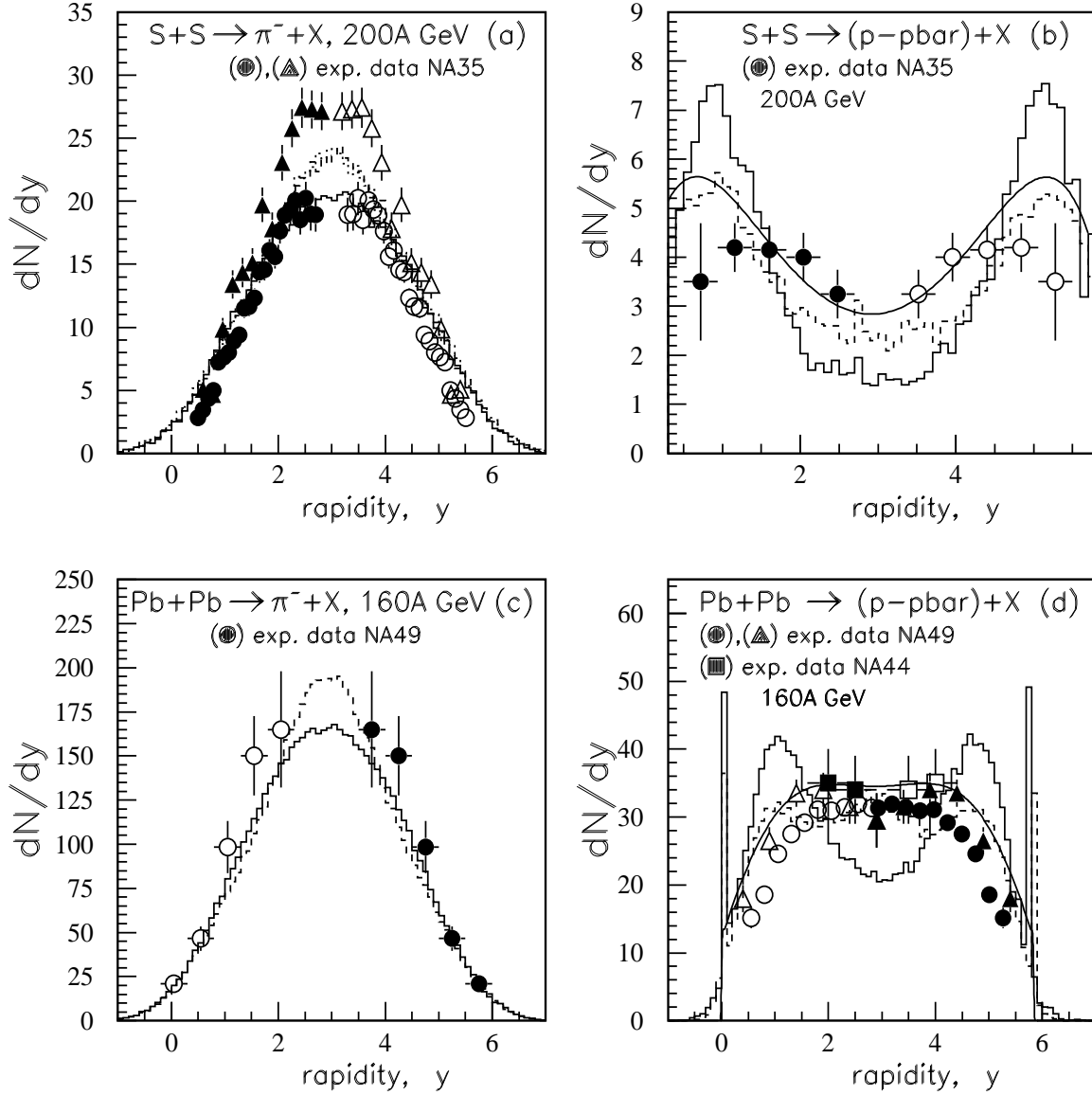


Figure 4: Comparison of central $S+S$ at 200 AGeV (a,b) NA35[1, 20] and central $Pb+Pb$ at 160 AGeV (c,d) (NA49[2, 12, 15] (solid triangles), NA44[3](solid squares)) data with calculations. Open circles and open squares are reflected data around mid-rapidity. New preliminary analysis[4] of $p - \bar{p}$ are shown by solid dots in part (d). Solid and dashed histograms correspond to HIJING[28] and VENUS[29] models, and continuous curves are predictions of the Multi-Chain Model [8].

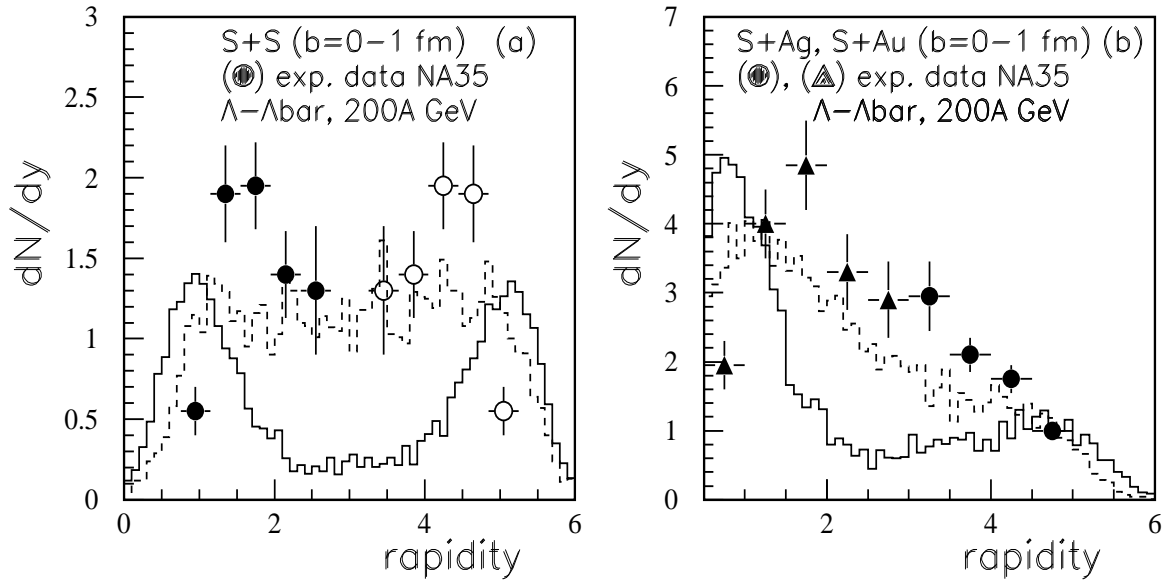


Figure 5: Net Hyperon $\Lambda - \bar{\Lambda}$ rapidity distributions in central $S + A$ at 200 AGeV (a,b) NA35[1]. Solid and dashed histograms correspond to HIJING[28] and VENUS[29] models.

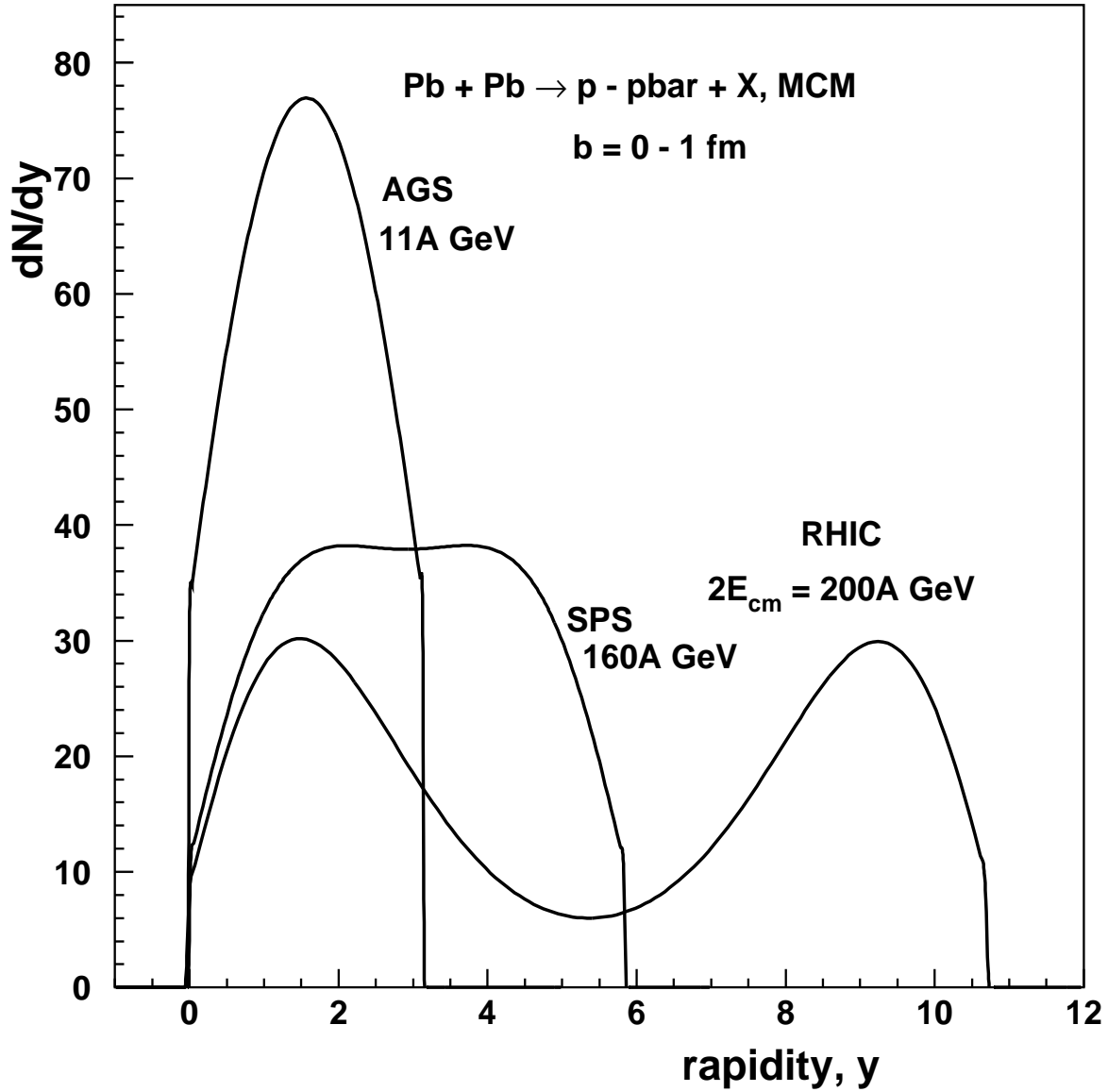


Figure 6: The energy dependence of the net positive baryon number transport in central $Pb + Pb$ reactions based on the MCM.

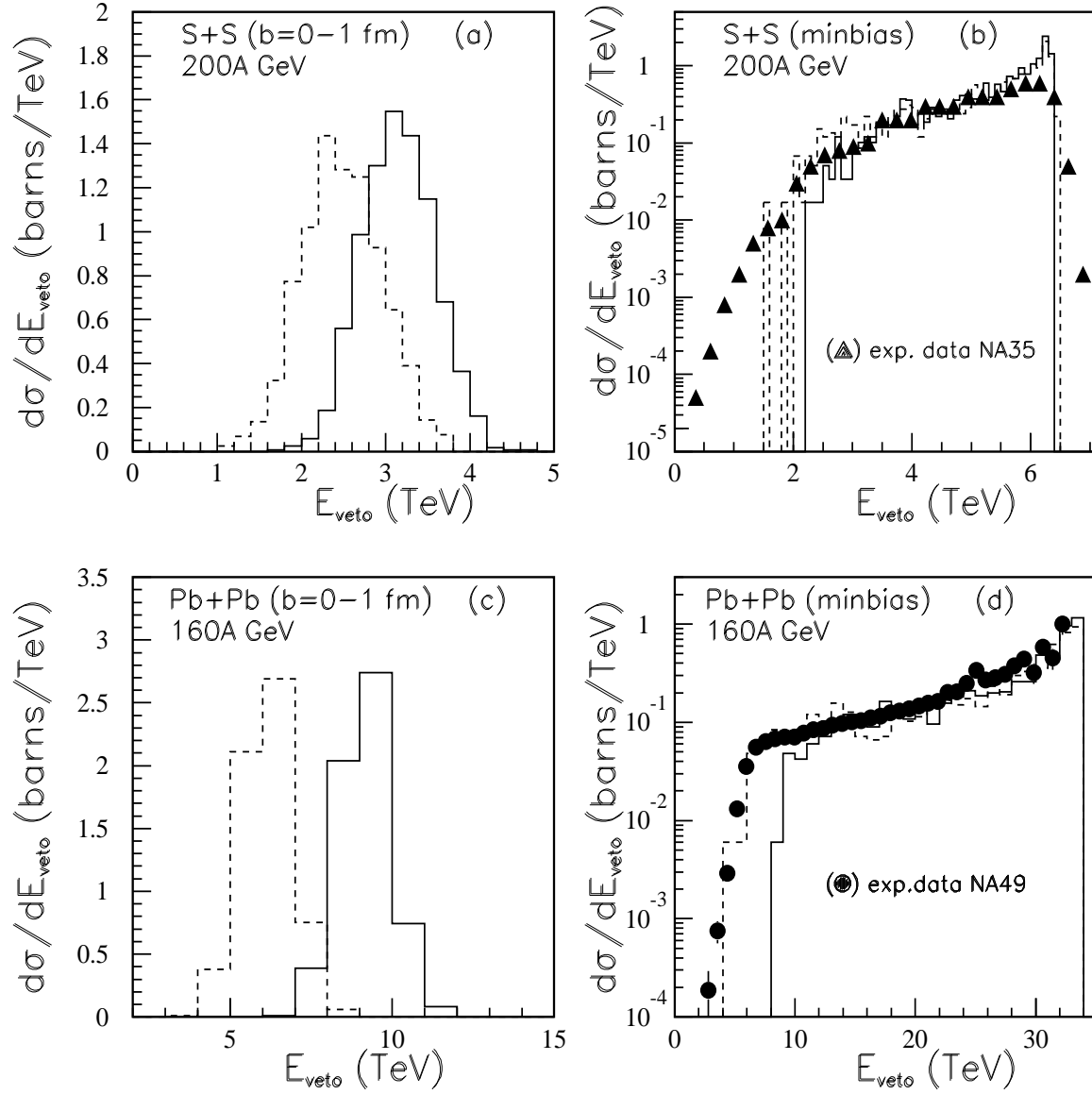


Figure 7: The veto calorimeter cross section in SS [14] and $Pb-Pb$ [15] collisions. Solid and dashed histograms refer to HIJING and VENUS models.

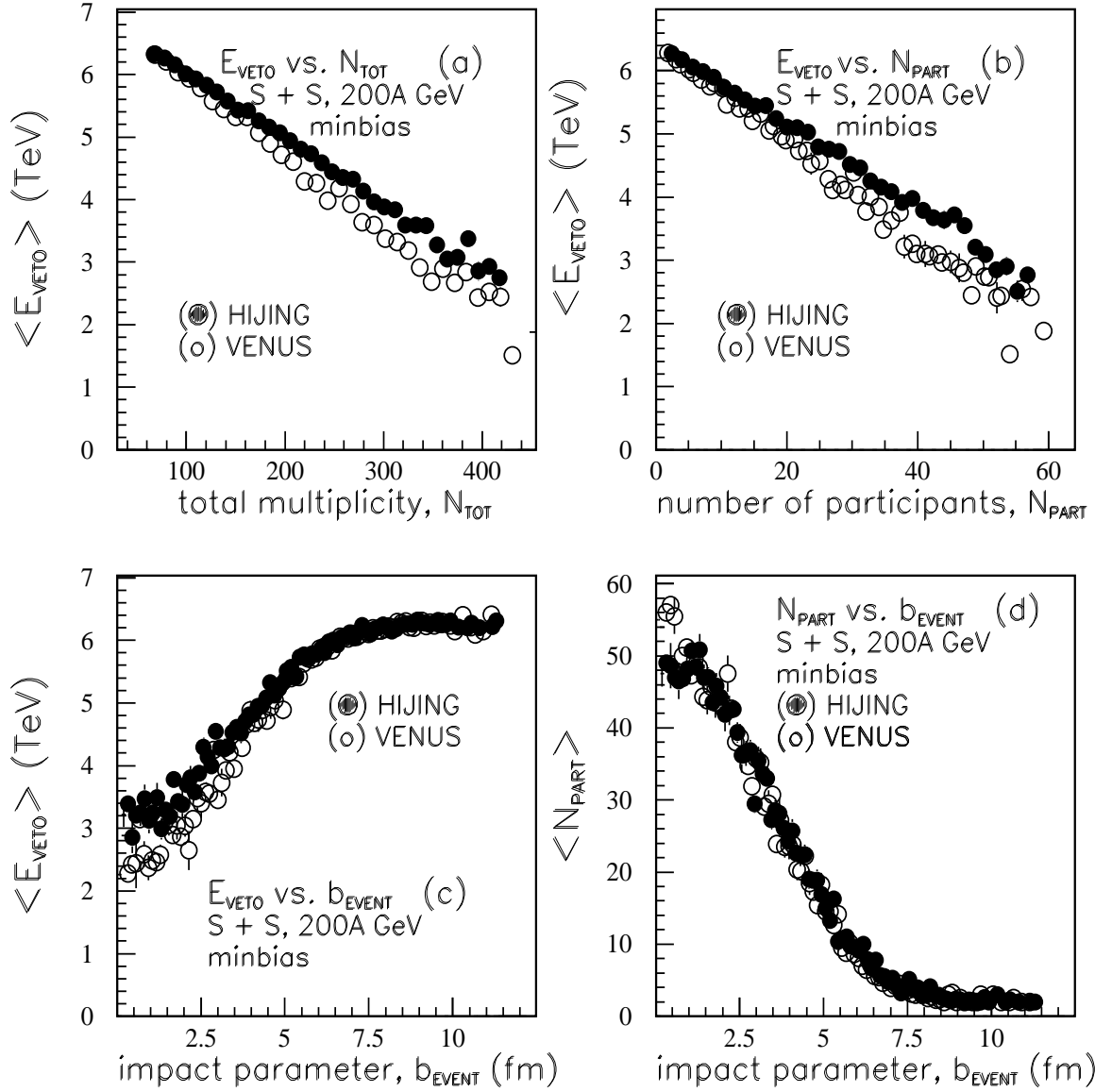


Figure 8: Dependence of the mean E_{VETO} as a function of (a) the total multiplicity, (b) number of participant (or wounded) nucleons, and (c) impact parameter in $S + S$ reactions comparing HIJING (solid) and VENUS (open) models. Part (d) shows the mean participant number as a function of impact parameter.

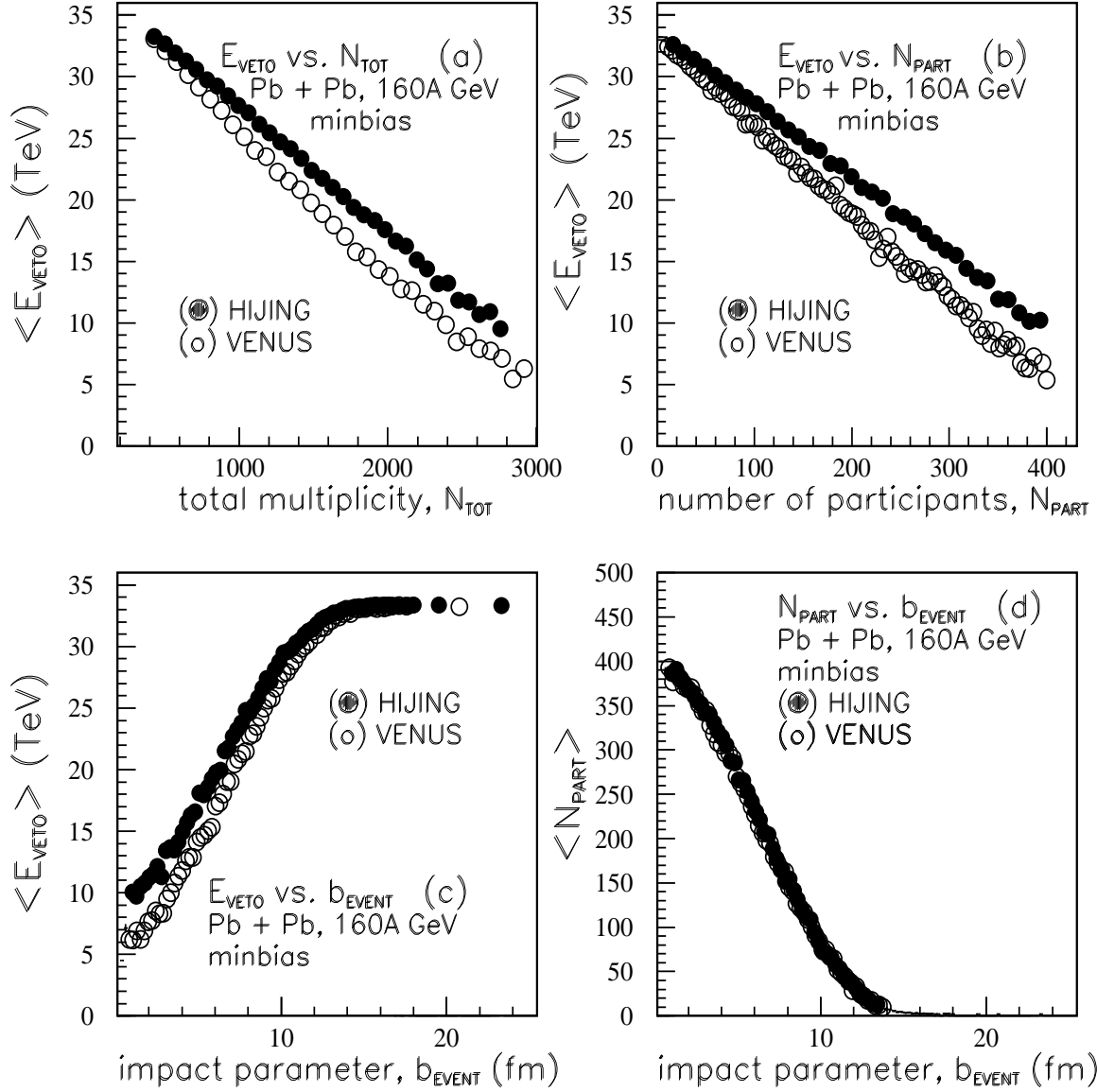


Figure 9: Dependence of the mean E_{VETO} as a function of (a) the total multiplicity, (b) number of participant (or wounded) nucleons, and (c) impact parameter in $Pb + Pb$ reactions comparing HIJING (solid) and VENUS (open) models. Part (d) shows the mean participant number as a function of impact parameter.

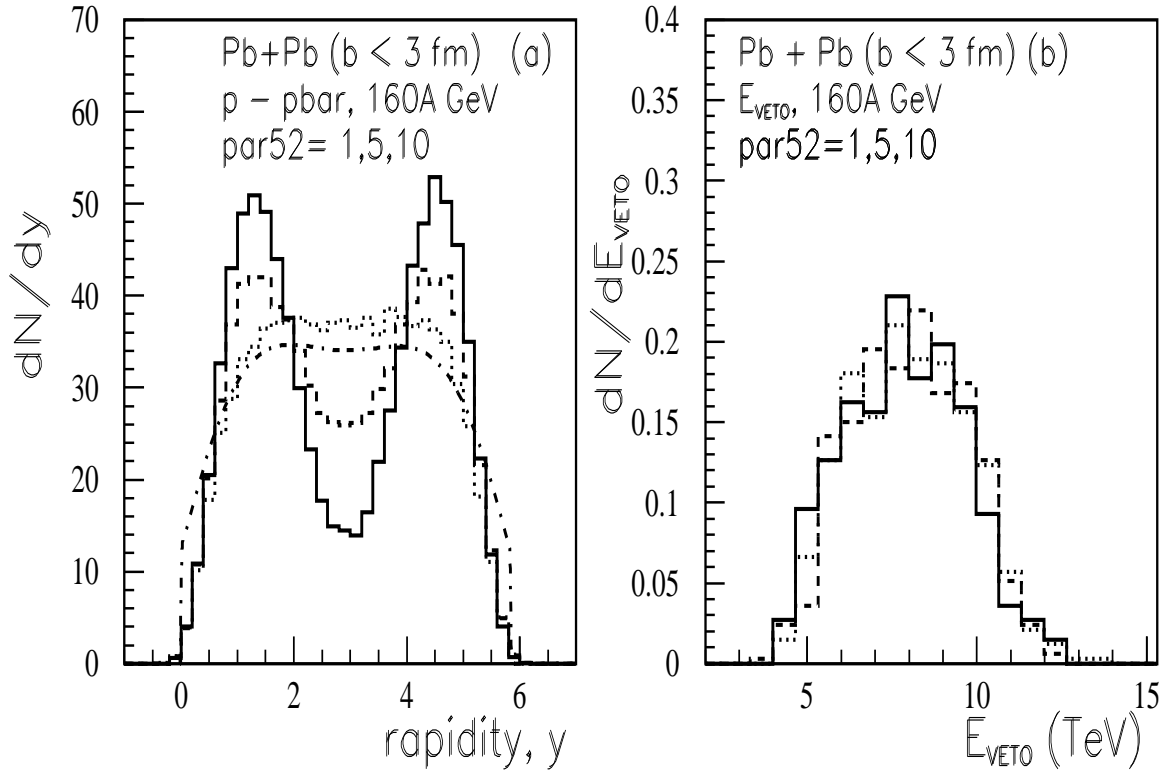


Figure 10: (a) Variation of baryon transport using the ATTILA[41] version of Fritiof[26]. The effect of changing the parameter $p = par(52)$ in the jetset6.3[40] diquark fragmentation scheme is shown. The default (solid) with $p = 1$, and modified $p = 5$ dashed and $p = 10$ dotted histograms are shown compared to the MCM prediction[8] as in Fig. 4d. (b) The veto calorimeter cross sections and hence energy degradation are uncorrelated to the baryon number transport in this model.